CHIN. PHYS. LETT. Vol. 37, No. 9 (2020) 097801

Phase-Gradient Metasurfaces Based on Local Fabry–Pérot Resonances

Yanyan Cao(曹燕燕)[1], Bocheng Yu(余博丞)[1], Yangyang Fu(伏洋洋)[2], Lei Gao(高雷)[1*], and Yadong Xu(徐亚东)[1*]

[1]*School of Physical Science and Technology, Soochow University, Suzhou 215006, China*
[2]*College of Science, Nanjing University of Aeronautics and Astronautics, Nanjing 211106, China*

(Received 29 June 2020; accepted 3 August 2020; published online 1 September 2020)

In this work, we present a new mechanism for designing phase-gradient metasurfaces (PGMs) to control an electromagnetic wavefront with high efficiency. Specifically, we design a transmission-type PGM, formed by a periodic subwavelength metallic slit array filled with identical dielectrics of different heights. It is found that when Fabry–Pérot (FP) resonances occur locally inside the dielectric regions, in addition to the common phenomenon of complete transmission, the transmitted phase differences between two adjacent slits are exactly the same, being a nonzero constant. These local FP resonances ensure total phase shift across a supercell, fully covering a range of 0 to 2π, satisfying the design requirements of PGMs. Further research reveals that, due to local FP resonances, there is a one-to-one correspondence between the phase difference and the permittivity of the filled dielectric. A similar approach can be extended to the reflection-type case and other wavefront transformations, creating new opportunities for wave manipulation.

PACS: 78.67.Pt, 42.79.Dj, 42.25.Gy DOI: 10.1088/0256-307X/37/9/097801

In recent years, great effort has been devoted to both the theoretical and experimental study of electromagnetic (EM) phase-gradient metasurfaces (PGMs),[1–5] due both to their fundamentally interesting characteristics, and to the practical importance of PGMs, such as the generalized Snell law (GSL),[6] and metalenses.[7] Typically, PGMs are constructed as periodic gratings, consisting of a supercell, spatially repeated along an interface, where each supercell consists of m unit cells (i.e., meta-atoms), with m being an integer. The key concept of PGMs is to introduce an abrupt phase shift covering the range of 0 to 2π discretely through m unit cells of different optical responses, so as to ensure complete control of the outgoing wavefront. The phase-gradient provides a new degree of freedom for the manipulation of light propagation, which has resulted in the construction of a series of ultrathin devices to realize anomalous scattering,[8] the photon spin Hall effect,[9] and other phenomena.[10–12]

The most common method of introducing the required abrupt phase shift takes advantage of the resonance of a resonator, as the phase shift between the emitted and incident radiation of an optical resonator changes appreciably across a resonance. For instance, a metallic V-shaped antenna was designed in pioneering work in the field of PGMs,[6] whereby the required abrupt phase shift, covering the range of 0 to 2π, was introduced discretely by eight antennas (i.e., $m = 8$) by engineering the total length and the angle between the rods. Based on different physical mechanisms, the choice of resonators varies widely, from plasmonic nanostructures[13] to metal-dielectric hybrid structures such as the so-called Huygens meta-atoms[14–16] and high-index dielectric cylinders or blocks,[17,18] and the operating frequencies involved vary from the microwave range to the mid-infrared and visible range.

In this work, we suggest an alternative approach to introducing the abrupt phase shift required for the design of PGMs. In particular, we design and study a transmission-type metallic grating, consisting of a periodic subwavelength metallic slit array filled with *identical* dielectrics of different heights, which we call metallic metagrating for convenience. In fact, this structure, or something similar to it, designed for wavefront control, has been discussed extensively in previous works,[8,19–21] in which phase accumulation on the geometric path is used to introduce the required abrupt phase shift at the outgoing interface. Here, in contrast to all previous results, we show that adjusting the height of each dielectric facilitates a series of Fabry–Pérot (FP) resonances in the transmission spectrum which do not happen in the whole structure, but occur *locally* inside the dielectric regions. These *local* FP resonances result in the transmitted phase

Supported by the National Natural Science Foundation of China (Grant Nos. 11974010, 11604229 and 11774252), the Natural Science Foundation of Jiangsu Province (Grant Nos. BK20161210 and BK20171206), the China Postdoctoral Science Foundation (Grant No. 2018T110540), the Qinglan Project of Jiangsu Province of China (Grant No. BRA2015353), and the Priority Academic Program Development (PAPD) of Jiangsu Higher Education Institutions.
*Corresponding authors. Email: leigao@suda.edu.cn; ydxu@suda.edu.cn
© 2020 Chinese Physical Society and IOP Publishing Ltd

differences between two adjacent slits being exactly the same, and the total phase shift covers the range from 0 to 2π, fully satisfying the design requirements of PGMs. This mechanism has never been found before. Interestingly, we also find that such transmitted phase differences, related to the integer number m for the PGM design, are only determined by the permittivity of the dielectric filled inside the slits.

Intuitively, the number of unit cells m in a supercell does not influence PGM diffraction characteristics, except that a small value of m will lead to a reduced diffraction efficiency.[18] However, some recent studies have shown that the integer m plays a fundamental role in determining the high-order PGM diffractions[21] when the incident angle is beyond the critical angle predicted by GSL.[6] In particular, for high-order PGM diffractions, m leads to a new set of diffraction equations expressed as:[21]

$$\begin{aligned} k_x^{\mathrm{i}} &= k_x^{\mathrm{r}} + nG, \quad L = \text{even}, \\ k_x^{\mathrm{i}} &= k_x^{\mathrm{t}} + nG, \quad L = \text{odd}, \end{aligned} \tag{1}$$

where $k_x^{\mathrm{i}} = k_0 \sin\theta_{\mathrm{i}}$ and $k_x^{\mathrm{r(t)}} = k_0 \sin\theta_{\mathrm{r(t)}}$ represent the tangential wave vectors of the incident and reflected (refracted or transmitted) waves, $G = 2\pi/p$ is the reciprocal lattice vector, n is the diffraction order, and $L = m - n$ is the propagation number of multiple internal total reflections inside the PGM, i.e., the number of times that the wave travels inside the PGM. Such an additional process of multiple internal total reflections can lead to angularly asymmetric absorption[22–25] in a PGM, with some loss, because absorption efficiency is also related to m. Therefore, in addition to the phase gradient, the integer number of unit cells m in a supercell is another degree of freedom, which can be employed to control the light propagation. This work is also related to the integer m. We show that local FP resonances lead to a one-to-one relationship between the integer m and the permittivity of the filled dielectric, such that a specific transmitted phase difference automatically meets the design requirements of the PGM in terms of m. In other words, for a fixed value of m, there is always a specific permittivity, such that the PGM design can realize wavefront control. An analytical expression for this relationship is presented below, thereby providing a new way to manipulate an EM wavefront.

Figure 1(a) shows a schematic diagram of the PGM studied in this work; the metallic grating consists of periodically repeated supercells, with a period length of p, and a thickness of h. Each supercell includes m unit cells with identical widths of $a = p/m$, and each unit cell is made of metal silver (gray areas), perforated by a slit filled with the same nonmagnetic dielectric (orange areas) with a permittivity of ε_{d}. The slit width is w, and the dielectric height in the ith unit cell is d_i $(i = 1, \ldots, m)$. A transverse-magnetic (TM) polarized light, with its magnetic field operating only along the z direction, is incident from air onto this PGM. Based on the concept of PGMs,[6,8] the transmitted phase retardation across a supercell should fully cover the range from 0 to 2π, and the phase difference between two adjacent unit cells is $\Delta\phi = 2\pi/m$, which defines a phase gradient of $\xi = \Delta\phi/\Delta x = 2\pi/p$.

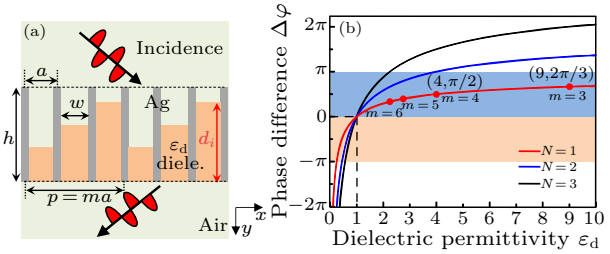

Fig. 1. (a) Schematic diagram of the designed transmission-type metagrating, with a supercell consisting of m unit cells. The orange and gray areas represent the dielectric and metal, respectively. To introduce the required abrupt phase shift at the transmission interface, the slits are filled with identical dielectrics of different heights. (b) Transmitted phase difference $\Delta\varphi$ between two adjacent unit cells versus the permittivity ε_{d} of the filled dielectric for $N = 1$ (red curve), 2 (blue) and 3 (black). For $N = 1$, the red solid circles in the curve indicate the required specific value of ε_{d} for designing a PGM with m.

Prior to further discussion, we first consider the transmission characteristics of ordinary periodic metallic slit arrays (PMSAs), filled with dielectrics of the same height d. By performing numerical calculations based on COMSOL multiphysics, Fig. 2(a) shows the relationships between the transmission phase retardation and amplitude vs the thickness d for normal incidences. In calculations, the operating wavelength is $\lambda = 3\,\mu\mathrm{m}$, $h = 2\,\mu\mathrm{m}$, $a = 1\,\mu\mathrm{m}$, $f = w/a = 0.8$ and $\varepsilon_{\mathrm{d}} = 9$. Note that a and f will not significantly affect the phase shift profile if $w \ll \lambda$.[26] As illustrated by Fig. 2(a), increasing d leads to a series of pronounced FP resonances with perfect transmission (i.e., $T = 1$). This result is obvious in typical FP resonances. However, unusually, the transmitted phase varies monotonically and almost linearly as d increases [see the blue curve in Fig. 2(a)]. In particular, at the FP resonances, the phase differences between two adjacent resonances are exactly equidistant and exactly equal to $\Delta\varphi = 2\pi/3$. To further explain the FP resonances, Fig. 2(b) displays the numerically calculated magnetic field distributions of three FP resonances at $d = 0.48$, 0.97, and $1.46\,\mu\mathrm{m}$. The left panel shows the total magnetic field patterns in three different unit cells. It is clear that the FP resonances discussed above do not originate from the *overall behavior* of the grating structure, or the collective behavior of individual silts, but occur locally in the dielectric regions. The right panel of Fig. 2(b) plots the line distributions of the magnetic fields at the center position, in-

dicated by the dashed line in the left panel. The black curves represent the magnitude of the magnetic field; the red, green, and blue curves represent the phase of the magnetic field. The orange areas indicate the interior of the dielectric materials. In three cases, the accumulated phases of the EM field across the dielectric regions, as indicated by the colored circles, are approximately π, 2π, and 3π, and feature the typical characteristics of FP resonances, thereby confirming that the FP resonances occur locally only inside the dielectrics.

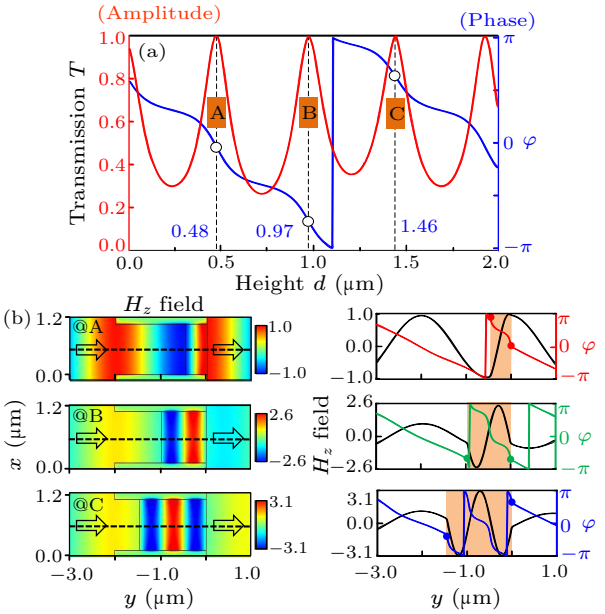

Fig. 2. Local FP resonances lead to equal phase differences. (a) The relationships between the transmission T (left axis) and transmitted phase φ (right axis) vs the height d of identical dielectrics with $\varepsilon_d = 9$ filled in ordinary periodic metallic slit arrays (PMSAs). The transmitted phase φ is almost linearly varying, and the phase difference between two adjacent FP resonances is constant at $2\pi/3$. (b) Magnetic field distribution in a unit cell where FP resonances occur, which from top to bottom correspond to $d = 0.48$, 0.97, and 1.46 μm. The left panel shows the field pattern for each FP resonance, and the right panel plots the line distribution of the magnetic field along the centerline, indicated by the dashed line in the left panel. Here $\lambda = 3$ μm and $h = 2$ μm.

The phase difference between the two adjacent FP resonances is $\Delta\varphi = 2\pi/3$. Such a phase difference is exactly the phase difference between two adjacent unit cells required for the design of a PGM with $m = 3$ unit cells in a supercell, i.e., $\Delta\phi = 2\pi/m$. To test this point, we design a PGM with $\xi = k_0$ by assembling the three unit cells shown above with different heights together, in a metallic metagrating, as shown in Fig. 1(a). In this case, because $m = 3$ is odd, the outgoing direction of the EM wave for arbitrary incidence is governed by $k_x^{\rm i} = k_x^{\rm t} + nG$ with $n = -1$, when $\theta_i < 0°$, corresponding to the lowest-order diffraction (i.e., the GSL), and $k_x^{\rm i} = k_x^{\rm r} + nG$ when $\theta_i > 0$, corresponding to higher-order diffraction.[21]

Figure 3(a) shows the calculated diffraction efficiency of each diffraction order of the designed metallic metagrating for full incidence, ranging from $-90°$ to $90°$. When $\theta_i < 0°$, the anomalous transmission of the lowest diffraction order is dominant (i.e., $n = -1$, blue solid line), and the efficiency reaches 99.7% at $\theta_i = -30°$. When $\theta_i > 0°$, due to the odd $m = 3$, the outgoing wave exhibits an anomalous reflection for the high order ($n = 1$, red dotted line), and the efficiency is 99.3% at $\theta_i = 30°$. Figures 3(b) and 3(c) show the total magnetic fields corresponding to the incident angles $\theta_i = -30°$ and $30°$, respectively. The black arrows indicate the directions of the incidence and anomalous transmission/reflection. The magnetic field pattern clearly shows that a metallic metagrating can achieve near-perfect anomalous wavefront control. All these results are perfectly consistent with previous research[21] where impedance-matched materials with different refractive indices are required.

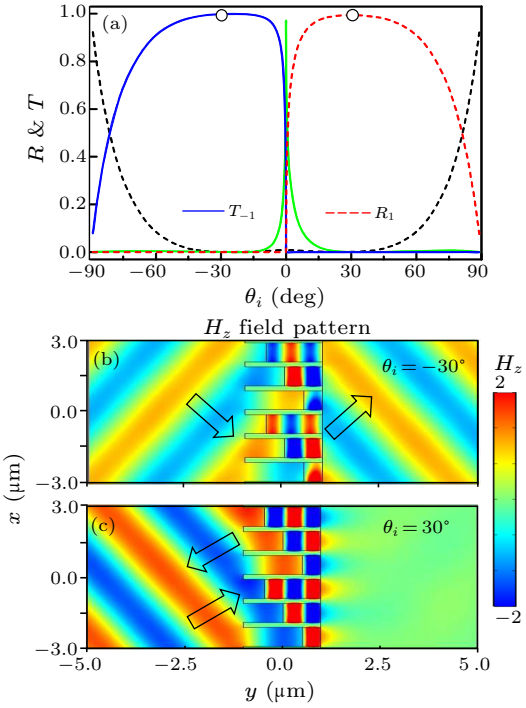

Fig. 3. Design of a PGM with $m = 3$, and its performance. (a) Diffraction efficiency (transmission T or reflection R) of diffraction orders $n = -1$ (blue curve) and 1 (red curve). [(b), (c)] Magnetic field patterns for $\theta_i = -30°$ and $\theta_i = 30°$, respectively. Here the phase gradient is $\xi = k_0$, which means that $p = \lambda = 3$ μm, and $a = 1$ μm.

In fact, this phenomenon is not accidental, but involves profound physics. A one-to-one relationship exists between the integer number of unit cells m and the permittivity ε_d. To further examine this relationship, for simplicity, we consider a normally incident TM wave from air onto the metagrating used in this work. Once the EM wave passes through the ith slit and reaches the transmission interface, the total phase retardation is approximately given by $\varphi_i = k_0(h - d_i) +$

$\sqrt{\varepsilon_{\rm d}}k_0d_i+\varphi_0$,[26] where φ_0 is an additional phase originating from the multiple reflections at the interface between the metagrating and the air, and is the same for all slits in a supercell. Note that, due to $w \ll \lambda$, only the fundamental mode generally exists inside the subwavelength slits, and its propagation constant is given by $\varepsilon_{\rm m}\sqrt{\beta^2-\varepsilon_{\rm r}k_0^2}\tanh\left(\sqrt{\beta^2-\varepsilon_{\rm r}k_0^2}w/2\right) = -\varepsilon_{\rm r}\sqrt{\beta^2-k_0^2\varepsilon_{\rm m}}$,[8] where $\varepsilon_{\rm m}$ and $\varepsilon_{\rm r}$ are the relative permittivities of the metal (silver) and the medium filled inside the slits. In our case, the operating wavelength of $\lambda = 3\,\mu$m leads to $\beta \approx k_0$ for the air region ($\varepsilon_{\rm r} = 1$) and $\beta \approx \sqrt{\varepsilon_{\rm d}}k_0$, for the dielectric region ($\varepsilon_{\rm r} = \varepsilon_{\rm d}$). Similarly, when the wave passes through the adjacent $(i+1)$th slit, $\varphi_{i+1} = k_0(h-d_{i+1})+\sqrt{\varepsilon_{\rm d}}k_0d_{i+1}+\varphi_0$. At the transmission interface, the phase difference between two adjacent slits is then expressed as:

$$\Delta\varphi = \varphi_{i+1}-\varphi_i = k_0(d_i-d_{i+1})+\sqrt{\varepsilon_{\rm d}}k_0(d_{i+1}-d_i). \tag{2}$$

When the FP resonances occur in the dielectric region (i.e., not in the air region) in all slits, $\sqrt{\varepsilon_{\rm d}}k_0d_i = j\pi$ and $\sqrt{\varepsilon_{\rm d}}k_0d_{i+1} = j'\pi$, where j and j' are integers with arbitrary values. These local FP resonances will lead to $\sqrt{\varepsilon_{\rm d}}k_0(d_{i+1}-d_i) = N\pi$, with the integer $N = j-j'$, which is also an arbitrary integer. This means that when the wave passes through the adjacent dielectric materials, the transmitted phase difference is also an integer multiple of π. Substituting these results into Eq. (2) yields

$$\Delta\varphi = N\pi(1-1/\sqrt{\varepsilon_{\rm d}}). \tag{3}$$

This is due to the fact that the PGMs require the phase differences between two adjacent unit cells to be $\Delta\phi = 2\pi/m$, $\Delta\phi = \Delta\varphi$, which produces the following relationship:

$$\varepsilon_{\rm d}(m) = \left[mN/(mN-2)\right]^2. \tag{4}$$

Equation (4) implies that the permittivity of the filled dielectric is only determined by integers m and N. In particular, when N is fixed, one can obtain a one-to-one relationship between the filled medium and the integer number of unit cells m. In other words, for a fixed value of m, there is always a specific dielectric constant, such that the PGM design is able to realize wavefront control.

Based on Eq. (3), Fig. 1(b) plots the relationships between the transmitted phase difference and the permittivity $\varepsilon_{\rm d}$, where the red, blue, and black colors correspond to $N = 1$, 2, and 3, respectively. Due to $m \geqslant 2$ in the PMG design, $|\Delta\phi| \leqslant \pi$. Therefore, we must only consider the range of $-\pi \leqslant \Delta\varphi \leqslant \pi$ in Fig. 1(b), which can be divided into two sections: $0 < \Delta\varphi \leqslant \pi$ (the blue region), and $-\pi \leqslant \Delta\varphi < 0$ (the red region). The two sections correspond to two phase gradients in opposite directions. Here, for simplicity, we take $N = 1$ as an example to illustrate the permittivity $\varepsilon_{\rm d}$ for different values of m, and only consider the case of $0 < \Delta\varphi \leqslant \pi$, which leads to $\varepsilon_{\rm d} \geqslant 1$. For a PGM with $m = 3$, $\Delta\phi = 2\pi/3$. Based on Fig. 1(b) or Eqs. (3) and (4), $\Delta\varphi = \Delta\phi = 2\pi/3$ corresponds to $\varepsilon_{\rm d} = 9$. More generally, as indicated by the red solid circle in Fig. 1(b), for other values of m, such as $m = 4$, 5, and 6, the required permittivity is $\varepsilon_{\rm d}(4) = 4$, $\varepsilon_{\rm d}(5) = 25/9$, and $\varepsilon_{\rm d}(6) = 9/4$, respectively. In an extreme case, when the transmitted phase difference is $\Delta\varphi \to 0$ (i.e., m tends to infinity), $\varepsilon_{\rm d}(m) \to 1$. In this case, the PGM is reduced to a common PMSA. In other words, as long as $m \geqslant 2$, a value of $\varepsilon_{\rm d}$ will always exist, as predicted by Eq. (4), that can that satisfies the design requirements of the PGM.

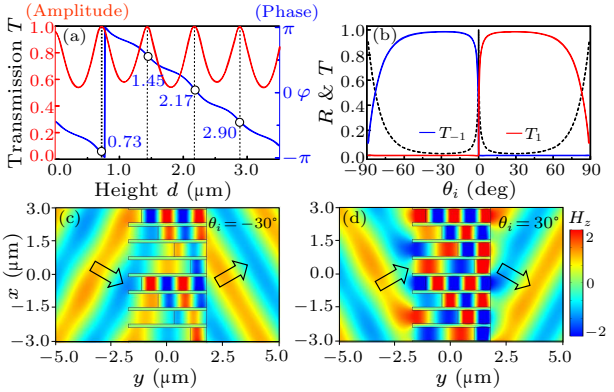

Fig. 4. Design for a PGM with $m = 4$ and its performance. The required dielectric permittivity is $\varepsilon_{\rm d} = 4$. (a) The relationships between the transmission T (left axis) and transmitted phase φ (right axis) vs the height d of identical dielectrics, with $\varepsilon_{\rm d} = 4$ filled in ordinary metallic slit arrays (PMSAs). (b) Diffraction efficiency (transmission T or reflection R) of diffraction orders $n = -1$ (red curve) and 1 (blue curve). [(c), (d)] Magnetic field patterns for $\theta_i = -30°$ and $\theta_i = 30°$, respectively. Here, the operating wavelength is still $\lambda = 3\,\mu$m, and the phase-gradient is $\xi = k_0$, which means that $p = \lambda = 3\,\mu$m, and $a = 0.75\,\mu$m.

The revealed physics of the local FP resonances, together with the associated analytical formulas of Eqs. (2)–(4) provide guidance for the design of PGMs with arbitrary m. To further clarify the correctness of our proposal, we design and explore an alternative PMG with even $m = 4$, which is related to $\varepsilon_{\rm d} = 4$, based on Eq. (4), when $N = 1$. As above, let us first examine the transmission properties of a common PMSA filled with identical dielectrics with $\varepsilon_{\rm d} = 4$; the calculated results are shown in Fig. 4(a). For consistency with the parameters of the PGM designed below, in the calculations, $\lambda = 3\,\mu$m, $a = 0.75\,\mu$m, and $f = w/a = 0.8$. The grating height is changed to $h = 3.5\,\mu$m in order to achieve more local FP resonances. As shown by the red transmission curves, with d ranging from 0 to 3.5 μm, there are four peaks with

perfect transmission ($T = 1$) at $d = 0.73$, 1.45, 2.17, and 2.90 μm, due to the FP resonances locally occurring inside the dielectric regions. The blue curve shows the corresponding transmitted phase, with four circles indicating the FP positions. Clearly, the phase differences between two adjacent resonances are exactly equidistant and exactly equal to $\Delta\varphi = \pi/2$.

Moreover, a PGM with $\xi = k_0$ is designed by simply assembling these four unit cells together. Figure 4(b) shows the calculated diffraction efficiency of all possible diffraction orders for the designed metallic metagrating with $m = 4$. Note that because m is even, the outgoing direction of the EM wave for arbitrary incidence is governed by $k_x^{\mathrm{i}} = k_x^{\mathrm{t}} + nG$, with $n = -1$ when $\theta_i < 0$, corresponding to the lowest-order diffraction (i.e., the GSL), and $k_x^{\mathrm{i}} = k_x^{\mathrm{t}} + G$ when $\theta_i > 0$, corresponding to higher-order diffraction.[21] The calculated results in Fig. 4(b) are consistent with this diffraction law. It can be seen that when $\theta_i < 0°$, the transmission is dominated by the lowest order $n = -1$ (see the blue curve), and when $\theta_i = -30°$, the efficiency is $T_{-1} = 98.5\%$. When $\theta_i > 0°$, the transmission is dominated by the higher order $n = 1$ (see the red curve), and the efficiency is $T_1 = 98.5\%$ at $\theta_i = 30°$. To highlight the performance of the wavefront transformation, Figs. 4(c) and 4(d) illustrate the magnetic field pattern for $\theta_i = -30°$ and $\theta_i = 30°$, respectively. Perfect negative refractions can be observed for both incidences, and their outgoing directions completely follow the results predicted by the new set of diffraction laws. Therefore, the designed metallic metagratings perform well in manipulating a wavefront with high or perfect efficiency.

So far, we have discussed and verified the correctness of Eq. (4), revealing a one-to-one relationship between the filled medium and the integer number of unit cells m. It should be noted that although the required medium for a certain m is rigorously determined by Eq. (4), for example, $\varepsilon_{\mathrm{d}} = 9$ for $m = 3$, the performance of the designed PGM is actually not very sensitive to variations in permittivity, as it is well-known that most PGMs have some degree of tolerance to abrupt phase shifts.[21] To illustrate this point, we take the case of $m = 3$ as an example, and for convenience we focus only on two dominated diffraction orders of $n = \pm 1$ in Fig. 3. Keeping all parameters in Fig. 3 unchanged, Fig. 5 presents the relationship between T_{-1} (R_1) at $\theta_i = -30°$ (30°) and the permittivity ε_{d} of the filled dielectric. It can be seen that at $\varepsilon_{\mathrm{d}} = 9$, an ideal value predicted by Eq. (4), the PGM exhibits perfect anomalous transmission/reflection; it maintains its performance level even as ε_{d} deviates slightly from the ideal value. For instance, for a deviation of 5% (see the two dashed lines), the diffraction efficiencies are still very high. Specifically, when $\varepsilon_{\mathrm{d}} = 8.55$, then $T_{-1} = 94.6\%$ and $R_1 = 96.3\%$, and when $\varepsilon_{\mathrm{d}} = 9.45$, then $T_{-1} = 93.0\%$ and $R_1 = 98.6\%$. Figures 5(b) and 5(c) show the corresponding field patterns for the two cases, from which one can observe that all wavefronts are effectively maintained. Therefore, the proposed PGM has a certain degree of flexibility in relation to variations in permittivity, which greatly relaxes the requirements in terms of experimentally implementing the PGM.

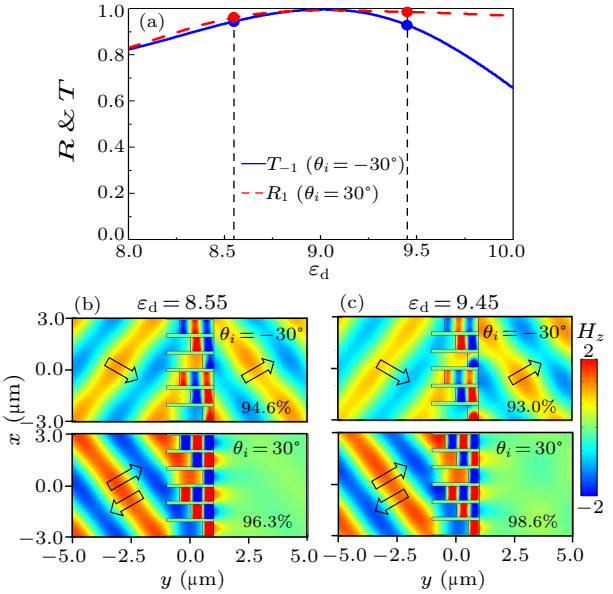

Fig. 5. Influence of permittivity variation on the performance of the proposed PGM, based on local FP resonances when $m = 3$. (a) Diffraction efficiency T_{-1} at $\theta_i = -30°$ and R_1 at $\theta_i = 30°$ vs the permittivity ε_{d} of the filled medium. Two black dashed lines indicate the positions of a 5% deviation from the ideal value of $\varepsilon_{\mathrm{d}} = 9$. [(b), (c)] Simulated field patterns for the case of $\varepsilon_{\mathrm{d}} = 8.55$ and $\varepsilon_{\mathrm{d}} = 9.45$, respectively. Here, all parameters are the same as those in Fig. (3), with the exception of the permittivity of the filled medium.

In summary, we have demonstrated a new strategy for designing a PGM to manipulate an EM wavefront with high efficiency. The configuration studied in this work is a transmission-type PGM, formed by a periodic subwavelength metallic slit array filled with identical dielectrics of different heights. We have found that the local FP resonances can produce exactly the same transmitted phase differences between two adjacent slits, and facilitate a total phase shift that fully covers the range of 0 to 2π, satisfying the design requirements for PGMs. More importantly, the equal phase difference is closely related to the permittivity of the filled dielectric; as a result, the local FP resonances lead to a one-to-one relationship between the permittivity and the integer number of unit cells, m, in a supercell of the PGM. Based on this strategy, two specific examples of PGMs with $m = 3$ and $m = 4$ have been designed, which exhibit effective performance in wavefront control. Therefore, the studied

metallic metagratings and the proposed analytical formulae provide a powerful tool for the design of high-efficiency PGMs. The results of this work can be extended to include the reflection-type case as well as other wavefront transformations, creating opportunities for extreme wave manipulation, e.g., in an omnidirectional reflector,[27] and multifunctional wavefront manipulation.[28]

In practice, due to the one-to-one relationship between the permittivity and the integer number of unit cells m, the selection of the dielectric constant is limited. At a specific working frequency, and for a specific m, the required permittivity predicted by Eq. (4), may not be found in natural materials. This limitation can be overcome by the use of metamaterials, which in principle can produce an arbitrary permittivity value.[29] However, the trade-off is that using metamaterials will make the designed PGM more complex.

References

[1] Estakhri N M and Alù A 2016 *J. Opt. Soc. Am. B* **33** A21
[2] Kildishev A V, Boltasseva A and Shalaev V M 2013 *Science* **339** 1232009
[3] Minovich A E, Miroshnichenko A E, Bykov A Y *et al.* 2015 *Laser & Photon. Rev.* **9** 195
[4] Xu Y, Fu Y Y and Chen H 2016 *Nat. Rev. Mater.* **1** 16067
[5] Yu N and Capasso F 2014 *Nat. Mater.* **13** 139
[6] Yu N, Genevet P, Kats M A *et al.* 2011 *Science* **334** 333
[7] Wang S M, Wu P C, Su V C *et al.* 2018 *Nat. Nanotechnol.* **13** 227
[8] Xu Y, Fu Y and Chen H 2015 *Sci. Rep.* **5** 12219
[9] Yin X, Ye Z, Rho J *et al.* 2013 *Science* **339** 1405
[10] Genevet P, Lin J, Kats M A *et al.* 2012 *Nat. Commun.* **3** 1278
[11] Cui T J, Qi M Q, Wan X *et al.* 2014 *Light: Sci. & Appl.* **3** e218
[12] Ni X, Wong Z J, Mrejen M *et al.* 2015 *Science* **349** 1310
[13] Sun S, He Q, Xiao S *et al.* 2012 *Nat. Mater.* **11** 426
[14] Pfeiffer C and Grbic A 2013 *Phys. Rev. Lett.* **110** 197401
[15] Wong Alex M H and Eleftheriades George V 2018 *Phys. Rev. X* **8** 011036
[16] Zhang L, Ding J, Zheng H *et al.* 2018 *Nat. Commun.* **9** 1481
[17] Arbabi A, Horie Y, Bagheri M *et al.* 2015 *Nat. Nanotechnol.* **10** 937
[18] Ra'di Y, Sounas D L and Alù A 2017 *Phys. Rev. Lett.* **119** 067404
[19] Marcus S W and Epstein A 2019 *Phys. Rev. B* **100** 115144
[20] Palm D, Dang Z and Rahm M 2019 *Sci. Rep.* **9** 10792
[21] Fu Y, Shen C, Cao Y *et al.* 2019 *Nat. Commun.* **10** 2326
[22] Li Y, Shen C, Xie Y *et al.* 2017 *Phys. Rev. Lett.* **119** 035501
[23] Wang X, Díaz-Rubio A, Asadchy V S *et al.* 2018 *Phys. Rev. Lett.* **121** 256802
[24] Shen C and Cummer S A 2018 *Phys. Rev. Appl.* **9** 054009
[25] Cao Y, Fu Y, Zhou Q *et al.* 2019 *Phys. Rev. Appl.* **12** 024006
[26] Shi H, Wang C, Du C *et al.* 2005 *Opt. Express* **13** 6815
[27] Qian E, Fu Y, Xu Y *et al.* 2016 *Europhys. Lett.* **114** 34003
[28] Fu Y, Cao Y and Xu Y 2019 *Appl. Phys. Lett.* **114** 053502
[29] Xu Y, Gu C, Hou B *et al.* 2013 *Nat. Commun.* **4** 2561